Pergamon

Bioorganic & Medicinal Chemistry 9 (2001) 453–464

BIOORGANIC & MEDICINAL CHEMISTRY

New Antimetastatic Hypoxic Cell Radiosensitizers: Design, Synthesis, and Biological Activities of 2-Nitroimidazole-acetamide, TX-1877, and its Analogues

Soko Kasai,[a] Hideko Nagasawa,[a] Mao Yamashita,[a] Mie Masui,[a] Hideki Kuwasaka,[a] Tomoko Oshodani,[a] Yoshihiro Uto,[a] Taisuke Inomata,[b] Shigenori Oka,[c] Seiichi Inayama[d,e] and Hitoshi Hori[a,*]

[a]*Department of Biological Science and Technology, Faculty of Engineering, The University of Tokushima, Minamijosanjimacho-2, Tokushima 770–8506, Japan*
[b]*Department of Radiology, Kochi Medical School, Kochi 783–0043, Japan*
[c]*Research & Development Center, Nagase & Co., Ltd., Hyogo 651–2241, Japan*
[d]*Institute of Oriental Medical Science, Tokyo 155–0032, Japan*
[e]*Keio University, School of Medicine, Tokyo 160–8582, Japan*

Received 24 July 2000; accepted 2 October 2000

Abstract—We designed, based on the molecular orbital (MO) calculation, synthesized, and evaluated the biological activities of the new antimetastatic hypoxic cell radiosensitizer, 2-nitroimidazole-acetamide, TX-1877, and its analogues. Each analogue has an electron-affinic imidazole group, an acetamide group and a certain hydrophilic group to control its biological effect, toxicity, and pharmacokinetics. In in vitro radiosensitization assay, most TX-1877 analogues, which have an electron affinity (EA) of more than 0.9 eV and partition coefficient (P) of more than 0.021, showed satisfactory enhancement ratios (ER > 1.60) at doses of 1 mM. On the other hand, imidazole analogues, such as TX-1908 (EA = 0.67 eV), TX-1910 (EA = −0.34 eV) and TX-1931 (EA = −0.37 eV), which have low electron affinities, had an ER of 1.31 or less. TX-1877 and KIN-806 effectively inhibited tumor regrowth when administered with irradiation in vivo at a dose of 0.4 mg/g. Tumor lung metastasis was inhibited by treatment with either TX-1877 or KIN-806 without irradiation at a dose of 0.4 mg/g. TX-1877 reduced markedly the mean number of metastatic lung nodules in comparison with KIN-806. Moreover, TX-1877 and KIN-806 enhanced macrophage and helper T lymphocyte infiltration for 3 weeks after drug treatment. TX-1877 shows a high EA value and has the C^2 of HOMO localizing on N-methylamide and the C^2 of LUMO localizing on 2-nitroimidazole group. The MO data might be useful for designing a bifunctional hypoxic cell radiosensitizer. TX-1877 and its analogues are potential antimetastatic hypoxic cell radiosensitizers, which would improve the efficiency of radiotherapy and quality of life in cancer treatment. © 2001 Elsevier Science Ltd. All rights reserved.

Introduction

A high rate of tumor cell proliferation increases oxygen consumption in tumor tissue. Furthermore, abnormalities of structure and function in tumor vessels lead to decreased oxygen delivery to tumor tissue,[1] which becomes hypoxic and resistant to radiation therapy and some chemotherapy.[2,3] Tumor hypoxia can be exploited for selective anticancer drug treatment using hypoxic cell cytotoxins or hypoxic cell radiosensitizers.[4]

Hypoxic cell radiosensitizers, as electron-affinic compounds, have oxygen-mimicking effects to tumor hypoxic cells and fix the radiation-induced damage in DNA or other molecules.[5] Misonidazole [MISO, 1-methoxy-3-(2-nitro-1*H*-imidazolyl)-2-propanol] (Fig. 1) is a well-known 2-nitroimidazole radiosensitizer. Tested in clinical trials, its development was discontinued because of dose-limiting side effects such as neurotoxicity.[6] Etanidazole (SR2508) [*N*1-(2-hydroxyethyl)-2-(2-nitro-1*H*-imidazolyl)acetamide] (Fig. 1) was 3 to 4 times less toxic than MISO, but had radiosensitizing activity comparable to MISO. However, a phase III randomized trial of radiotherapy of head and neck cancer with or without etanidazole has failed.[7] Recently, hypoxic cell radiosensitizers have been designed not to improve radiosensitizing activities and hydrophilicities but to

*Corresponding author. Tel.: +81-886-56-7514; fax: +81-886-56-9164; e-mail: hori@bio.tokushima-u.ac.jp

0968-0896/01/$ - see front matter © 2001 Elsevier Science Ltd. All rights reserved.
PII: S0968-0896(00)00265-0

have chemical and biological activities by introducing additional functional groups, such as alkylating groups or enzyme chelating groups, to their side-chain moieties.[8–10] On the other hand, tumor hypoxia induced the production of vascular endothelial growth factor (VEGF) mediating angiogenesis, which is essential for tumor progression and metastasis.[11,12] Therefore, the combination of radiosensitization and antiangiogenesis targeting of tumor hypoxia can be a powerful anticancer therapeutic. We have previously reported that the antiangiogenic hypoxic cell radiosensitizer, haloacetylcarbamoyl-2-nitroimidazole, showed strong antiangiogenic activity in chicken embryo chorioallantoic membranes (CAM) assay.[13] Furthermore, we developed a hypoxic cell radiosensitizer, KIN-806 [*N*1,*N*1-dimethyl-2-(2-nitro-1*H*-1-imidazolyl)acetamide, Ro 7-1052] (Fig. 1), which has cell-differentiation inducing, antimetastatic and immunopotentiating activities.[14–16] KIN-806 has electron-affinic nitroimidazole with an *N*,*N*-dimethylacetamide group in its side-chain. TX-1877 [*N*1-(2-hydroxyethyl)-*N*-1-methyl-2-(2-nitro-1*H*-imidazolyl)acetamide], which was designed based on the structure of KIN-806 as the lead compound, showed more hydrophilicity and stronger antimetastatic activity than KIN-806.[17] In this paper, we give a full account of the design, synthesis, MO calculation, and in vitro radiosenstizing activity of TX-1877 analogues, and the in vivo biological activities of TX-1877 in comparison with those of KIN-806.

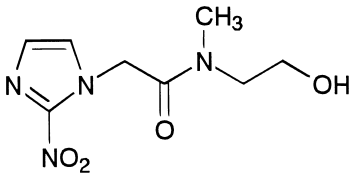

TX-1877

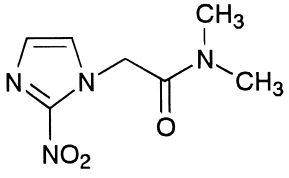

KIN-806

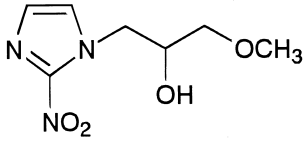

MISO

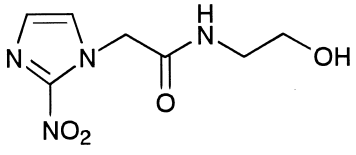

etanidazole

Figure 1. Structures of TX-1877, KIN-806, MISO, and etanidazole.

Results

Design and synthesis

The antimetastatic hypoxic cell radiosensitizer TX-1877 was designed based on the structure of KIN-806 to be more hydrophilic. TX-1877 has electron-affinic nitroimidazole with *N*-methylacetamide consisting of the hydroxyethylamine instead of *N*-methylamine of KIN-806 in its side-chain. TX-1877 has more potent in vivo antitumor and antimetastatic activities than KIN-806 (described below). We designed TX-1877 analogues, including *sec*-alcohol (TX-1902 and TX-1909), polyol (TX-1892 and TX-1904), ester (TX-1907 and TX-1911), morpholino (TX-1921), piperazino (TX-1920), and desoxy (TX-1914) analogues (Fig. 2).

TX-1877 was synthesized from methyl 2-(2-nitro-1*H*-1-imidazolyl)acetate (**1**), as a key intermediate, treated with *N*-methylethanolamine in anhydrous methanol for 26 h at room temperature, in 84% yield (Scheme 1). The ^{1}H NMR spectrum of TX-1877 showed that there were two resonance forms of *N*-methyl amide at room temperature. The *sec*-alcohol and polyol analogues, TX-1902, TX-1909, and TX-1892, were synthesized from **1** treated with their appropriate amines in methanol at room temperature in 72, 85 and 88% yield, respectively. Though TX-1904 was not afforded in the same condition, it was obtained in 71% yield by adding the potassium carbonate at 30–35 °C. Ester analogues, such as TX-1907 and TX-1911, were synthesized from TX-1877 using anhydrous acetic acid or pyridine–sulfur trioxide complex in dry pyridine in 91 and 78% yield, respectively. Syntheses of the morphorino, piperazino, and desoxy analogues, TX1921, TX-1920, and TX-1914, were performed using the corresponding neat amines (4–16 mol eq.) at room temperature in 83, 79, and 91% yield, respectively. Imidazole analogues, such as TX-1908, TX-1910, and TX-1931, were synthesized from the corresponding methyl esters **2**, **3** and **4** with *N*-methylethanolamine in 86, 56, and 51% yield, respectively. In the syntheses of **2** and **3**, imidazole and 4-methylimidazole were decomposed by using sodium methoxide, whereas they were obtained when other bases, such as triethylamine and potassium *tert*-butoxide, were used, as shown in Scheme 1. Most TX-1877 analogues were synthesized in good yields, and their structures and purities were identified based on physical and spectral data obtained by ^{1}H NMR, FTIR, and HRMS. Structures and melting points of these compounds are shown in Fig. 2 and Table 1. The partition coefficients were measured to estimate their toxicities and pharmacokinetics (Table 1).[18]

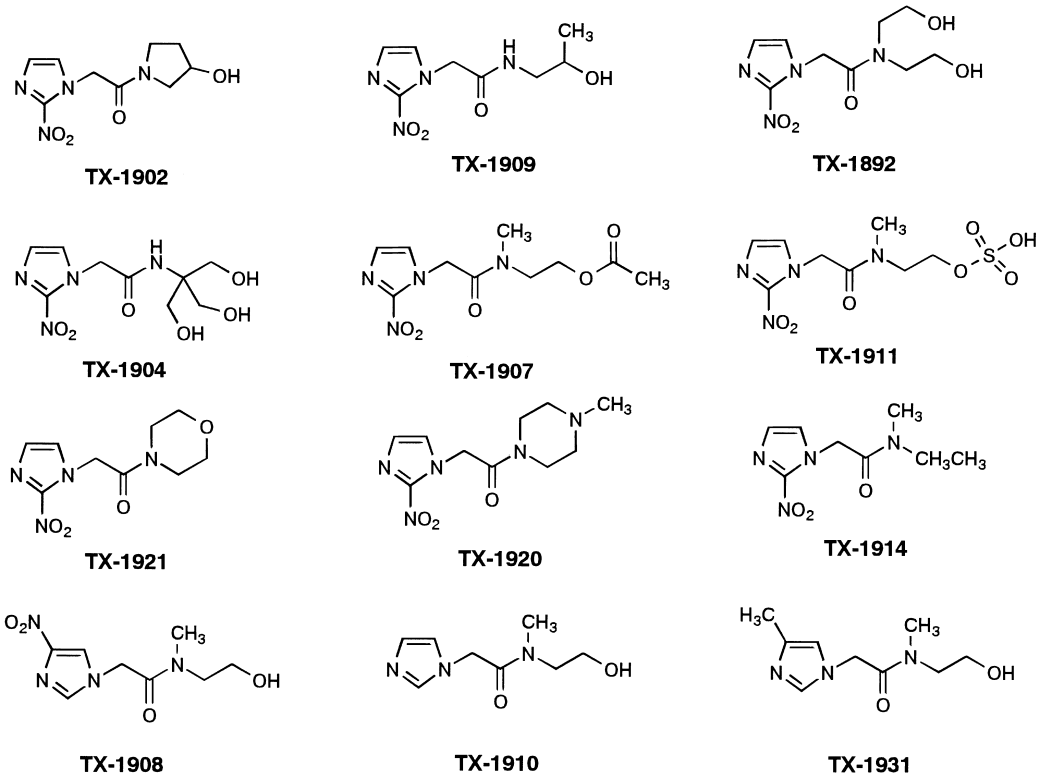

Figure 2. Structures of hypoxic cell radiosensitizer TX-1877 analogues.

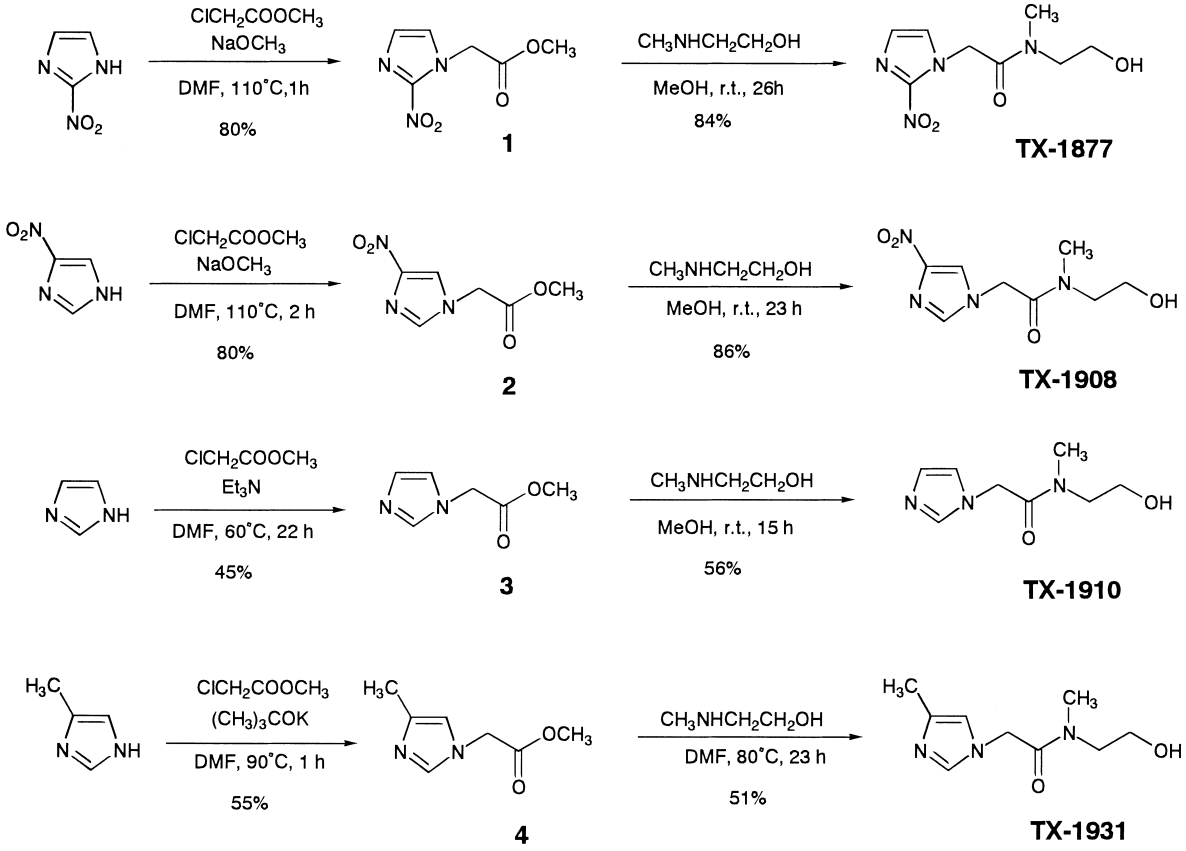

Scheme 1. Syntheses of 2-nitroimidazole hypoxic cell radiosensitizers TX-1877, TX-1908, TX-1910 and TX-1931.

Molecular orbital calculation

Electron affinity is an indicator of radiosensitizing activity as well as hydrophobicity.[19] We previously reported that the electron affinity [EA = −LUMO (the lowest unoccupied MO)] determined by MO calculation correlated with the radiosensitizing activity.[20] To predict their hypoxic cell radiosensitizing activities, we calculated the LUMO energy values (Eigen values) and measured partition coefficients (P) of TX-1877 analogues (Table 1). The EAs depended on the heteroaromatic groups of radiosensitizers. The EAs of 2-nitroimidazole analogues of TX-1877 were more than 0.9 eV and that of 4-nitroimidazole analogue (TX-1908) was 0.67 eV. On the other hand, the desnitroimidazole analogue (TX-1910) and 4-methylimidazole analogue (TX-1931) had EAs as low as −0.34 and −0.37 eV, respectively. We also calculated the square of atomic orbital coefficients (C^2) of LUMO and HOMO (the highest occupied MO) of TX-1877 analogues to estimate the effects of MO on biological activity (see Experimental). The C^2 values of TX-1877, KIN-806, TX-1910 and TX-1931 are depicted in their respective molecular diagrams (Fig. 3).

The C^2 value of LUMO of TX-1877 is higher on the 2-nitroimidazole group (N1: 0.189, C2: 0.169, N3: 0.154, C4: 0.04, C5: 0.195, and NO_2: 0.128) than that on the amide group of the side-chain. KIN-806 also showed the distribution of LUMO (N1: 0.189, C2: 0.170, N3: 0.153, C4: 0.04, C5: 0.195, and NO_2: 0.128) on the 2-nitroimidazole group. In both compounds, the sums of the C^2 values of LUMO on 2-nitroimidazole were 0.96 out of a total C^2 value of LUMO of 1.0 for the whole molecule, whereas the sums of C^2 values of HOMO on the N-methylamide group were 0.77 and 0.80 in TX-1877 and KIN-806, respectively. The sum of C^2 values of LUMO on the 4-nitroimidazole group was 0.86 in TX-1908. On the other hand, the desnitroimidazole analogue (TX-1910) had higher C^2 values of LUMO on the N-methylamide group (Me: 0.046, C (carbonyl): 0.475, N: 0.072, O: 0.012) and the total value was 0.60, while it was as low as 0.047 was on the imidazole ring. Similarly, the 4-methylimidazole analogue (TX-1931) had higher C^2 values of LUMO on the N-methylamide group (Me: 0.046, C (amide): 0.475, N: 0.072, O: 0.240) with a total of 0.83. The distribution of C^2 values of HOMO showed a trend opposite to that of LUMO in all compounds. It was remarkable that TX-1920, which had the highest ER (1.94), showed C^2 values of HOMO as high as 0.71 on the N-methyl nitrogen of piperazine.

Table 1. Physical data and in vitro radiosensitizing activities of TX-1877 analogues

Compound	Mp (°C)	P[a]	ER[b] (1 mM)	EA[c] (eV)	E_{pc}[d] (mV)
KIN-806	130–130.5	0.16	1.91	0.94	–
TX-1877	83–85	0.056	1.75	1.00	−661 (−449)
TX-1892	58–60	0.021	1.29	1.06	–
TX-1902	159–160	0.053	1.61	1.00	–
TX-1904	108–110	0.013	1.31	1.07	−664 (−452)
TX-1907	63–65	0.74	1.66	0.94	–
TX-1909	94–96	0.064	1.50	1.13	–
TX-l911	81–89	0.002	1.11	1.09	–
TX-1914	62–63	0.32	1.76	0.92	–
TX-1920	Amorphous	0.645	1.94	0.99	–
TX-1921	114–115	0.612	1.87	1.04	–
MISO	113–114[e]	0.422[e]	1.72[e]	0.93	−653 (−441)
Etanidazole	165–166[e]	0.048[e]	1.72[e]	1.16	−641 (−429)
TX-1908	112–113	0.051	1.31	0.67	−793 (−581)
TX-1910	123–125	0.017	1.18	−0.34	n.d.[f]
TX-1931	119–120	0.088	0.89	−0.37	n.d.[f]

[a]Partition coefficient (*n*-octanol/water) measured at pH 7.4 (0.1 M phosphate).
[b]For EMT6/KU cells at the dose of 1 mM.
[c]Electron affinit, $EA = -E_{LUMO}$ (eV).
[d]The cathodic peak potential (E_{pc}) was evaluated versus Ag/AgCl. Parentheses represent the potentials versus NHE (normal hydrogen electrode), E(NHE) = E(Ag/AgCl) + 212 mV.
[e]Data from ref 14.
[f]n.d., not determined due to the absence of electric response.

Electrochemical measurements of TX-1877 analogues

Cyclic voltametry (CV) was performed with TX-1877 analogues in an aqueous solution containing 0.1 M phosphate buffer (pH = 7.4)–0.5% (v/v) DMSO, and the obtained cathodic peak potentials versus Ag/AgCl expressed as E_{pc} were as follows: −661 mV for TX-1877, −664 mV for TX-1904, −641 mV for etanidazole, −653 mV for MISO, −793 mV for TX-1908, and no peak for TX-1910 and TX-1931, respectively (Table 1). All of the 2-nitroimidazole analogues were found to have similarly high reduction potentials (−641 to −664 mV), suggesting that they were reduced with electron transfer reaction more easily than 4-nitro (TX-1908), 4-methyl (TX-1931), and desnitroimidazole (TX-1910) analogues.

Radiosensitizing activity

In vitro radiosensitizing activities of TX-1877 analogues were measured at doses of 1 mM in EMT6/KU single cells under hypoxic conditions. The enhancement ratios (ERs) and the partition coefficients of TX-1877 analogues are shown in Table 1. Radiosensitizing activities of KIN-806 (ER = 1.91), TX-1877 (ER = 1.75), TX-1902 (ER = 1.61), TX-1907 (ER = 1.66), TX-1914 (ER = 1.76), TX-1920 (ER = 1.94), and TX-1921 (ER = 1.87) were comparable to MISO (ER = 1.72). Polyol analogues such as TX-1892 (ER = 1.29) and TX-1904 (ER = 1.31), and sulfonate TX-1911 (ER = 1.11) have low radiosensitizing activity, because of their higher hydrophilicities ($P < 0.02$). These results showed that in vitro ERs of most compounds were related to their partition coefficients except for 4-nitro, desnitro, and 4-methylimidazole analogues, such as TX-1908 (ER = 1.31), TX-1910 (ER = 1.18), and TX-1931 (ER = 0.89).

Tumor growth inhibition and antimetastatic activity of TX-1877 and KIN-806

Tumor growth inhibition by TX-1877 and KIN-806 is shown in Figure 4. TX-1877 with R (radiation) and KIN-806 with R efficiently suppressed tumor regrowth

at 20 days after the treatment (0.4 mg/g). The tumor volume of TX-1877 without R was slightly reduced but that of KIN-806 was not reduced. In the group only irradiated, tumor regrowth was observed 9 days after the treatment, whereas tumor regrowth for TX-1877 with R was not observed (data not shown). Antimetastatic activity of TX-1877 and KIN-806 is shown in Figure 5. TX-1877 and KIN-806 reduced the mean numbers of metastatic lung nodules even without irradiation and they markedly reduced the mean numbers

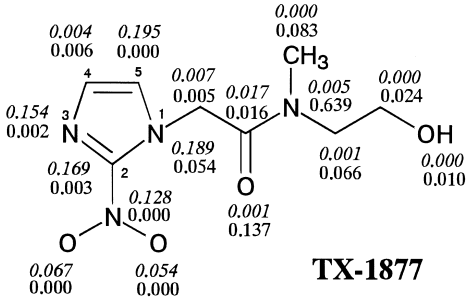

E_{LUMO} = -1.004 eV
E_{HOMO} = -10.162 eV
Total energy = -2953.44597 eV

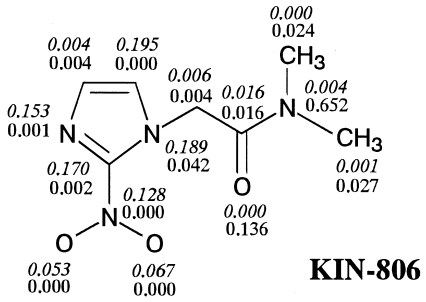

E_{LUMO} = -0.946 eV
E_{HOMO} = -10.043 eV
Total energy = -2510.27680 eV

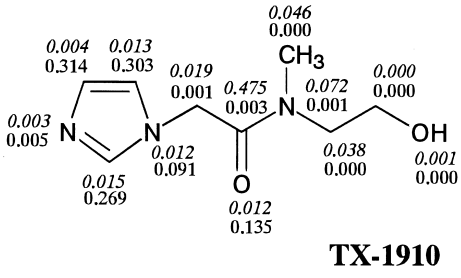

E_{LUMO} = 0.346 eV
E_{HOMO} = -9.415 eV
Total energy = -2222.06461 eV

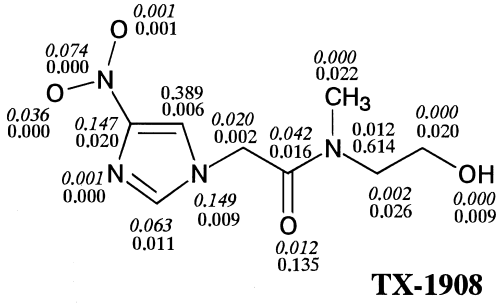

E_{LUMO} = -0.679 eV
E_{HOMO} = -10.410 eV
Total energy = -260.85534 eV

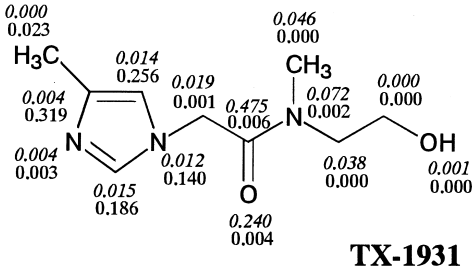

E_{LUMO} = 0.372 eV
E_{HOMO} = -9.132 eV
Total energy = -2371.782600 eV

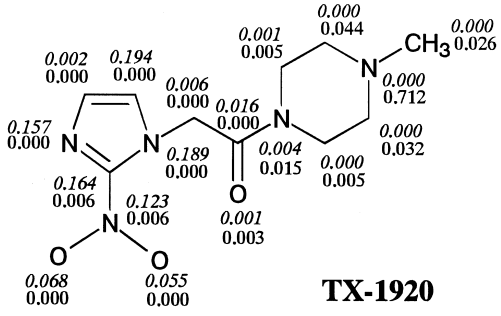

E_{LUMO} = -0.994 eV
E_{HOMO} = -9.459eV
Total energy = -52.79817 eV

Figure 3. The molecular diagram, orbital energy of LUMO (E_{LUMO}) and HOMO (E_{HOMO}), and total energy of hypoxic cell radiosensitizers TX-1877, KIN-806, TX-1908, TX-1910, TX-1931, and TX-1920. The C^2 values of LUMO (italic) and HOMO are shown in the molecular diagram.

of metastatic lung nodules within 22 days after the irradiation. TX-1877 has more potent antimetastatic activity than KIN-806 in the absence of irradiation.

Mononuclear cell infiltration in tumor tissue

Table 2 shows the intensity of the macrophage, B cell, helper T lymphocyte, and killer T cell infiltration in tumor tissue at 1, 2, and 3 weeks after the various treatments. Macrophage infiltration was moderately or markedly enhanced by TX-1877 (0.4 mg/g) and KIN-806 (0.4 mg/g) during 3 weeks after the treatment. When combined with radiation, macrophage infiltration was not detected at 1 week, because the tumor volume was too small. We considered that the macrophages contributed to antitumor activity. Helper T cell infiltration was slightly enhanced by TX-1877 and KIN-806, but helper T cell were not detected in control and following radiation of 30 Gy. Killer T cell infiltration was very slightly or moderately enhanced by TX-1877 and KIN-806, respectively. B cell infiltration was slightly or moderately enhanced by TX-1877 and KIN-806.

Discussion

Hypoxic cells in solid tumors not only are a major problem for radiation therapy but also lead to resistance to most anticancer drugs, accelerate malignant progression, and increase metastasis.[4,21] Therefore, hypoxic cells are important targets for cancer chemotherapy. The major goal of our research is to design low-toxicity bifunctional hypoxic cell radiosensitizers which have biological response modifier (BRM) activity, such as antimetastatic, antiangiogenic,[13] immunopotentiating as well as radiosensitizing activity. We previously designed a bifunctional hypoxic cell radiosensitizer KIN-806 which suppressed tumor metastasis and enhanced immunoresponse.[15,16] A new antimetastatic hypoxic cell radiosensitizer TX-1877 with an *N*-hydroxyethylamide group was designed to be more hydrophilic than KIN-806 with an *N*-methylamide group, although the in vitro radiosensitizing activity of TX-1877 (ER = 1.75) was higher than that of etanidazole (ER = 1.72), but lower than that of KIN-806 (ER = 1.91), as shown in Table 1. We expected that TX-1877 would not pass through the blood–brain barrier (BBB) because of its high hydrophilicity ($P = 0.056$) which was close to that of etanidazole ($P = 0.048$) and, therefore, show less neurotoxicity. In in vitro radiosensitization experiments, most 2-nitroimidazole analogues showed potent radiosensitizing activities (ER > 1.6) except highly hydrophilic compounds ($P \leqq 0.021$). TX-1911 showed the lowest radiosensitizing activity (ER = 1.11) among them, because it could be little incorporated into tumor cells due to hydrophilic sulfonate group. Similarly, hydrophilic polyol analogues, such as TX-1892 and TX-1904, also showed low ER values, 1.29 and 1.31, respectively. TX-1920, having an *N*-methylpiperazine group, had the highest radiosensitizing activity (ER = 1.94). Stratford et al. reported that weak basic hypoxic cell radiosensitizers were localized adjacent to the DNA due to their ionic interactions.[22] Because TX-1920 is a weak basic and hydrophobic compound (calculated $pK_a = 7.53$ and $P = 0.645$) and has a C^2 value of HOMO as high as 0.712 on the nitrogen of *N*-methylpiperazine (Fig. 3), it could be easily incorporated into tumor cells, thereby interacting with DNA.

The electron affinity measured by one-electron reduction potential or EA is thought to be an indicator of radiosensitizing activity as well as hydrophobicity.[19,20] We calculated the MO of TX-1877 analogues. All 2-nitroimidazole analogues showed high EAs between 0.92 and 1.16 eV. The radiosensitizing activities were mainly dependent on hydrophobicity when they had the same heteroaromatic group. The most hydrophobic TX-1920 ($P = 0.645$) gave the highest ER (1.94). We also designed 4-nitro- (TX-1908), desnitro- (TX-1910), and 4-methyl- (TX-1931) imidazole analogues with the same side-chain as TX-1877, which have lower electron affinities than 2-nitroimidazole analogues, to estimate the

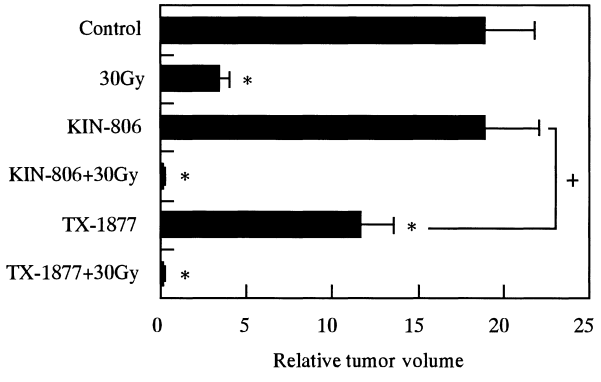

Figure 4. Relative volume of tumor treated with TX-1877 and KIN-806. TX-1877 (0.4 mg/g) and KIN-806 (0.4 mg/g) were administered to C3H/He mice (i.p.). The tumor volume was measured 20 days after the treatment. The relative tumor volume was compared to the tumor volume (1.00) at the beginning of the treatment. Each bar represents the mean ± s.d. for 15 mice. Statistical significance was determined using Student's *t* test. $^{*}p < 0.001$ versus control; $+p < 0.001$ versus KIN-806.

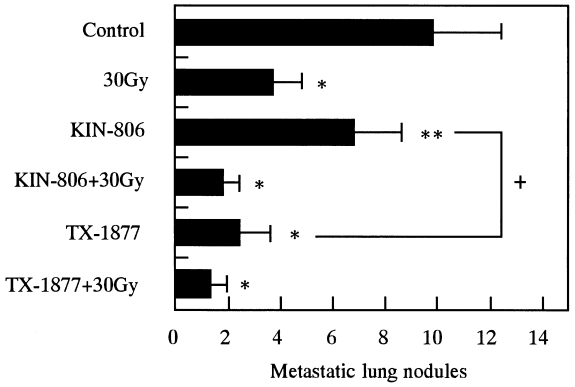

Figure 5. Metastatic lung nodules treated with TX-1877 and KIN-806. Metastatic lung nodules were counted 22 days after the treatment. TX-1877 (0.4 mg/g) and KIN-806 (0.4 mg/g) were administered to C3H/He mice (i.p.). Each bar represents the mean ± s.d. for 15 mice. Statistical significance was determined using Student's *t*-test. $^{*}p < 0.001$ versus control; $^{**}p < 0.002$ versus control; $+p < 0.001$ versus KIN-806.

influence of the heteroaromatic ring on their biological activities. Their ERs decreased with decreasing EA values. We also evaluated their reduction potentials as E_{pc} using cyclic voltametry. The data corroborated the results of MO calculation, which indicated that EA values were useful to predict the radiosensitizing activities instead of the reduction potentials (see Table 1). The C^2 values of LUMO of TX-1910 and TX-1931 shifted from their imidazole groups to the amide groups on their side-chain more than in 2-nitroimidazole analogues (Fig. 3). As a result of its decreased EA value and shift of C^2 values of LUMO to the amide group, TX-1931 (EA = −0.37 eV) showed radioprotective activity (ER = 0.89).

It was reported that the activation of macrophages by biological response modifier (BRM) played an important role in its antitumor activity.[23] TX-1877 and KIN-806 enhanced the mononuclear cell infiltration, especially macrophages, into the tumor tissue during 3 weeks after the drug treatment, as shown in Table 2. When combined with radiation, TX-1877 reduced the tumor growth for 3 weeks and enhanced macrophage infiltration at 3 weeks after irradiation. Although the mechanisms of antimetastatic activities of TX-1877 and KIN-806 are not completely elucidated, they may be related to their immunopotentiating activities. Recently, Kagiya et al. reported that nitrotriazole-type hypoxic cell radiosensitizer AK-2123 [*N*1-(2-methoxyethyl)-2-(3-nitro-1*H*-1,2,4-triazol-1-yl)acetamide] had antimetastatic and immunopotentiating activities acting as a BRM, which enhanced NK cells, macrophages, and other lymphocytes, and then suppressed the tumor metastasis.[24,25] On the other hand, it was reported that MISO and etanidazole promoted the formation of metastasis of Lewis lung carcinoma and B16 melanoma cells to the lungs and other organs in C57BL mice.[26] Although TX-1877 and KIN-806 are very similar to etanidazole in chemical structure and EA, they inhibited the lung metastasis without radiation in vivo. It was reported that the polar solvent, *N*-methylformamide (NMF), had antitumor[27] and immunopotentiating[28] activities. It was suggested that the *N*-methyl-amide group of TX-1877 and KIN-806 plays a role in their antimetastatic activity. Previously, it was reported that a chemically reactive species was formed by oxidative metabolism of *N*-methyl group.[29,30] The C^2 value of HOMO on the *N*-methyl carbon of TX-1877 and KIN-806 was 0.083 and 0.024, respectively. These results suggested that the *N*-methyl group of TX-1877 is more susceptible to oxidative metabolism than that of KIN-806. TX-1877 and KIN-806 exhibited antimetastatic activities, but the desnitroimidazole analogue (TX-1910) did not (data not shown). TX-1910 had higher C^2 values of LUMO on its amide group (C: 0.475, N: 0.072, O: 0.012) and higher values of HOMO on its imidazole group (N1: 0.091, C2: 0.269, N3: 0.005, C4: 0.314, CS: 0.303), which showed the reverse relationship between the amide group and the nitroimidazole group of TX-1877 and KIN-806 (see Fig. 3). This indicated that the *N*-methyl group of TX-1910 was hard to oxidize. Therefore, the MO data might be useful for the rational design of bifunctional hypoxic cell radiosensitizers having antimetastatic and immunopotentiating activities. We are examining antimetastatic activities of various analogues to investigate the MO and activity relationships. The minimum requirements for a hypoxic cell radiosensitizer are a high EA (> 0.9 eV) and localized C^2 of LUMO on the electron-deficient heteroaromatic group, and for BRM, presumably, localized C^2 of HOMO on a functional group of the side-chain. We will further evaluate the antiangiogenic activities of other TX-1877 analogues and also examine the relationship between the antimetastatic and immunopotentiating activities of TX-1877 analogues.

Conclusion

In the present study, we designed, based on the MO calculation, and synthesized new antimetastatic hypoxic cell radiosensitizer TX-1877 analogues. Almost all the TX-1877 analogues showed potent in vitro radiosensitizing activities. TX-1877 and KIN-806 inhibited

Table 2. Mononuclear cell infiltration in tumor tissue at 1, 2, and 3 weeks after the treatment. TX-1877 (0.4 mg/g) and KIN-806 (0.4 mg/g) were administered i.p.[a]

Week	Control	30 Gy	KIN-806	KIN-806 + 30 Gy	TX-1877	TX-1877 + 30 Gy
Macrophage						
1	—	*	+ +	*	+ +	*
2	+	+	+ + +	*	+ + +	+ + +
3	—	+	+ +	+ +	+ + +	+ + +
B cell						
1	±	*	+	*	+	*
2	±	+	+ +	*	+	+
3	—	+	+ +	—	+	+
Helper T cell						
1	—	*	+	*	+	*
2	—	—	±	*	+	—
3	—	—	±	+ +	±	—
Killer T cell						
1	+	*	+ +	*	+ +	*
2	±	±	+	*	+	—
3	+	±	+	+	±	—

[a]*Tumor volume was too small to be estimated. −: No infiltration; ±: Very slight; +: Slight; + +: Moderate; + + +: Marked.

tumor lung metastasis and enhanced infiltration by macrophages without irradiation. TX-1877 has remarkable antimetastatic activity. TX-1877 has a high EA, a moderate *P* value, large C^2 values of HOMO on *N*-methylamide, and large C^2 values of LUMO on 2-nitroimidazole group. These observations suggested that the MO calculation data might be useful for the design of bifunctional hypoxic cell radiosensitizers. Thus, TX-1877 is expected to have clinical applications as a bifunctional hypoxic cell radiosensitizer with antimetastatic and immunopotentiating activities. Furthermore, we will elucidate the antimetastatic activities of TX-1877 analogues and design more potent TX-1877 analogues.

Experimental

General procedures

^{1}H and ^{13}C NMR spectra were recorded on a JEOL JNM-EX400 spectrometer with tetramethylsilane as the internal standard. Chemical shifts are reported in ppm. Coupling constants are reported in Hz. IR spectra are recorded in KBr pellets on a Perkin–Elmer 1600 spectrometer. Mass spectra were measured on a Shimazu GC–MS QP-1000 mass spectrometer using an electron ionization (EI) method. High-resolution mass spectra (HRMS) were measured on a JEOL JMS-SX 102A mass spectrometer using a fast atom bombardment (FAB) and EI method. Reactions were monitored by analytical thin-layer chromatography (TLC) with use of Merck silica gel $60F_{254}$ glass plates and Merck aluminum oxide $60F_{254}$ neutral (Type E). Column chromatography was performed on Merck silica gel 60 (230–400 mesh) and aluminum oxide 90 active neutral (70–230 mesh). The *n*-octanol–water partition coefficient (*P*) was measured by Hitachi U-2000 spectrophotometer according to the method of Fujita et al.[31] All melting points were determined by Yanagimoto micro melting point apparatus (MP-S3 model) and are uncorrected. Elemental analysis was performed with a Yanako CHN recorder MT-5. All chemicals were purchased from Wako Pure Chemical Industries, Ltd. (Osaka, Japan), Kanto Chemical Co. Inc. (Tokyo, Japan), Tokyo Chemical Industry Co., Ltd. (Tokyo, Japan), and Sigma-Aldrich Japan (Tokyo, Japan). The semi-empirical molecular orbital (MO) calculation was applied by the PM3 methods of Stewart[32] and program MOPAC 97 (Fujitsu WinMOPAC V. 2.0, Fujitsu, Tokyo). Orbital energy (eV) of LUMO (E_{LUMO}) and HOMO (E_{HOMO}), C^2 value of LUMO and HOMO, and total energy (eV) were calculated. C^2 values of less than 0.05 were omitted. Electrodes for cyclic voltammetry (CV) were purchased from BAS (Osaka, Japan).

Synthesis of methyl 2-(2-nitro-1*H*-1-imidazolyl)acetate (1)

To a solution of 2-nitroimidazole (3 g, 26.5 mmol) in anhydrous DMF (20 mL), sodium methoxide (2 g, 37.0 mmol) was added at 90 °C. Chloroacetic acid methyl ester (3 g, 27.8 mmol) was added to the reaction mixture and stirred for 1 h at 100–110 °C. DMF was evaporated under reduced pressure, and the brown oil residue was purified by silica gel column chromatography (CH_2Cl_2:MeOH, 9:1) to afford **1** (4.2 g, 80%) as light yellow plates (from $CHCl_3$): mp 95–96 °C (lit.[33] mp 94–95); ^{1}H NMR (400 MHz, $CDCl_3$): δ 3.82 (s, 3H), 5.14 (s, 2H), 7.09 (s, 1H), 7.21 (s, 1H); IR (KBr) 3142, 3025, 2978, 1736, 1537, 1490, 1425, 1360, 1290, 1249, 1161, 1149, 984, 843, 784, 761, 696 cm^{-1}; EIMS *m*/*e*: 185 (M^+).

Synthesis of *N*1,*N*1-dimethyl-2-(2-nitro-1*H*-1-imidazolyl)-acetamide (KIN-806, Ro 7-1052)

To a solution of **1** (10 g, 54 mmol) in anhydrous MeOH (50 mL), *N*,*N*-dimethylamine in MeOH (112 mL, 270 mmol) was added. The reaction mixture was stirred for 18.5 h at room temperature. The solvent was evaporated under reduced pressure, and the residue was purified by silica gel column chromatography (CH_2Cl_2:MeOH, 99:1) to afford KIN-806 (9.3 g, 87%) as pale yellow needles (from acetone): mp 130–130.5 °C (lit.[33] mp 129–130); ^{1}H NMR (400 MHz, $CDCl_3$): δ 3.01 (s, 3H), 3.14 (s, 3H), 5.22 (s, 2H), 7.06 (s, 1H), 7.18 (s, 1H); IR (KBr) 3113, 2953, 2359, 1662, 1539, 1510, 1487, *1365,* 1301, 1161, 1138, 917, 843, 820, 794, 629 cm^{-1}; FABMS *m*/*e*: 199 (MH^+); HRMS (FAB^+) *m*/*e*: 199.0840 (MH^+ $C_7H_{11}O_3N_4$ requires 199.0831). MO data: $E_{LUMO=-0.946\,eV;}$ C^2 (LUMO): 0.195 (C-5, imidazole), 0.189 (N-1, imidazole), 0.170 (C-2, imidazole), 0.153 (N-3, imidazole), 0.128 (N, NO_2), 0.054 and 0.067(O, NO_2); $E_{HOMO} = -10.043$ eV; C^2 (HOMO): 0.625 (N, amide), 0.136 (O, amide); total energy: −2510.27680 eV.

Synthesis of *N*1-(2-hydroxyethyl)-*N*-1-methyl-2-(2-nitro-1*H*-imidazolyl)acetamide (TX-1877)

A solution of **1** (10.1 g, 50 mmol) and *N*-methylethanolamine (11.4 g, 152 mmol) in anhydrous MeOH (80 mL) was stirred for 26 h at room temperature. The solvent was evaporated under reduced pressure, and the residue was purified by silica gel column chromatography (CH_2Cl_2:MeOH, 8:2) to afford TX-1877 (9.7 g, 84%) as a light yellow solid: mp 100–102 °C; ^{1}H NMR (400 MHz, CD_3OD): δ 2.98 and 3.21 (each s, 3H) 3.50 and 3.66 (each t, $J = 5.6$ Hz, 2H), 3.55 and 3.79 (each t, $J = 5.2$ Hz, 2H), 5.43 and 5.54 (each s, 2H), 7.15 and 7.16 (each s, 1H), 7.37 and 7.40 (each s, 1H); ^{13}C NMR (100 MHz, CD_3OD): δ 34.26, 36.25, 51.98, 52.23, 52.42, 59.73, 60.43, 128.16, 129.04, 167.81, 168.14, 188.37; IR (KBr) 3549, 3124, 2929, 1661, 1532, 1487, 1470, 1367, 1292, 1206, 1160, 1137, 1068, 916, 845, 802, 632 cm^{-1}; HRMS (FAB^+) *m*/*e*: 229.0935 (MH^+ $C_8H_{13}O_4N_4$ requires 229.0892). MO data: $E_{LUMO} = -1.004$ eV; C^2 (LUMO): 0.195 (C-5, imidazole), 0.189 (N-1, imidazole), 0.169 (C-2, imidazole), 0.154 (N-3, imidazole), 0.128 (N, NO_2), 0.054 and 0.067 (O, NO_2); $E_{HOMO} = -10.154$ eV, C^2 (HOMO): 0.639 (N, amide), 0.137 (O, amide); total energy: −2953.44597 eV.

Synthesis of *N*1,*N*1-di(2-hydroxyethyl)-2-(2-nitro-1*H*-imidazolyl)acetamide (TX-1892, SR2555)

A solution of **1** (200 mg, 1.1 mmol) and 2,2′-iminodiethanol (350 mg, 3.3 mmol) in anhydrous MeOH

(8 mL) was refluxed for 24 h. The solvent was evaporated under reduced pressure, and the residue was purified by silica gel column chromatography (CH_2C1_2:MeOH, 9:1) to afford TX-1892 (250 mg, 88%) as a pale yellow solid: mp 78–79 °C (lit.[19] not described); ^{1}H NMR (400 MHz, CD_3OD): δ 3.52 (t, J = 5.6 Hz, 2H), 3.62 (t, J = 5.6 Hz, 2H), 3.67 (t, J = 5.6 Hz, 2H), 3.80 (t, J = 5.6 Hz, 2H), 5.55 (s, 2H), 7.15 (s, 1H), 7.32 (s, 1H) ; IR (KBr) 3397, 2943, 1649, 1542, 1500, 1425, 1374, 1295, 1216, 1160, 1142, 1073, 923, 843, 787, 650 cm^{-1}; HRMS (FAB$^+$) m/e: 259.0998 (MH^+ $C_9H_{15}O_5N_4$ requires 259.1023). MO data: E_{LUMO} = −1.062 eV; C^2 (LUMO): 0.194 (C-5, imidazole), 0.187 (N-1, imidazole), 0.161 (C-2, imidazole), 0.156 (N-3, imidazole), 0.132 (N, NO_2), 0.055 and 0.069 (O, NO_2); E_{HOMO} = −10.162 eV, C^2 (HOMO): 0.646 (N, amide), 0.147 (O, amide); total energy: −3396.68314 eV.

Synthesis of 1-(3-hydroxytetrahydro-1*H*-1-pyrrolyl)-2-(2-nitro-1*H*-1-imidazolyl)-1-ethanone (TX-1902)

To a solution of **1** (200 mg, 1.1 mmol) in anhydrous MeOH (7 mL), *dl*-3-pyrrolidinol (192 mg, 2.2 mmol) was added. The reaction mixture was refluxed for 23 h and then solvent was evaporated under reduced pressure, and the residue was purified by silica gel column chromatography (CH_2Cl_2:MeOH, 9:1) to afford TX-1902 (190 mg, 72%) as a white solid: mp 169–170 °C; ^{1}H NMR (400 MHz, CD_3OD): δ 1.89–2.12 (m, 2H), 3.23–3.45 (m, 2H), 3.49–3.68 (m, 2H), 4.36–4.48 (m, 1H), 5.25–5.37 (m, 2H), 7.10 (s, 1H), 7.35 (s, 1H); IR (KBr) 3339, 3128, 2955, 1659, 1542, 1497, 1457, 1422, 1371, 1142, 1103, 799 cm^{-1}; HRMS (FAB$^+$) m/e: 241.0938 (MH^+ $C_9H_{13}O_4N_4$ requires 241.0892). MO data: E_{LUMO}−1.005 eV; C^2 (LUMO): 0.182 (C-5, imidazole), 0.183 (N-1, imidazole), 0.139 (C-2, imidazole), 0.162 (N-3, imidazole), 0.162 (N, NO_2), 0.082 and 0.061 (O, NO_2); E_{HOMO} = −9.905 eV; C^2 (HOMO): 0.627 (N, amide), 0.134 (O, amide); total energy: −3072.15287 eV.

Synthesis of *N*1-[2-hydroxy-1,1-di(hydroxymethyl)-ethyl]-2-(2-nitro-1*H*-1-imidazolyl)acetamide (TX-1904)

To a solution of **1** (200 mg, 1.1 mmol) in anhydrous DMF (8 mL), 2-amino-2-hydroxymethyl-1,3-propandiol (240 mg, 2.2 mmol) and potassium carbonate (152 mg, 1.1 mmol) were added. The reaction mixture was stirred for 1.6 h at 30–35 °C, and then the solvent was evaporated under reduced pressure, and the residue was purified by silica gel column chromatography (CH_2Cl_2:MeOH, 8.8:1.2) to afford TX-1904 (215 mg, 71%) as a light yellow solid: mp 119–121 °C; ^{1}H NMR (400 MHz, CD_3OD): δ 3.75 (s, 6H), 5.21 (s, 2H), 7.16 (s, 1H), 7.41 (s, 1H); IR (KBr) 3428, 1683, 1542, 1494, 1368, 1295, 1161, 1140, 1051, 923, 843, 778, 650 cm^{-1}; HRMS (FAB$^+$) m/e: 275.0997 (MH^+ $C_9H_{15}O_6N_4$ requires 275.0947). MO data: E_{LUMO} = −1.074 eV; C^2 (LUMO): 0.194 (C-5, imidazole), 0.188 (N-1, imidazole), 0.163 (C-2, imidazole), 0.159 (N-3, imidazole), 0.131 (N, NO_2), 0.064 and 0.069(O, NO_2); E_{HOMO} = −10.039 eV; C^2 (HOMO): 0.588 (N, amide), 0.161 (O, amide); total energy: −3690.46747 eV.

Synthesis of 2-{methyl[2-(2-nitro-1*H*-1-imidazolyl)acetyl]-amino}ethyl acetate (TX-1907)

TX-1877 (500 mg, 2.2 mmol) was added to a solution of anhydrous acetic acid (300 mg, 7.9 mmol) and anhydrous pyridine (10 mL). The reaction mixture was stirred for 6.5 h, and then solvents were evaporated under reduced pressure. The residue was purified by silica gel column chromatography (CH_2Cl_2:MeOH, 9:1) to afford TX-1907 (542 mg, 91%) as a light yellow solid: mp 80–82 °C; ^{1}H NMR (400 MHz, $CDCl_3$): δ 2.05 and 2.15 (each s, 3H), 3.01 and 3.18 (each s, 3H), 3.62–3.67 (m, 2H), 4.22 and 4.30 (each t, J = 6.0 Hz, 2H), 5.21 and 5.32 (each s, 2H), 7.05 and 7.07 (s, 1H), 7.17 (s, 1H); IR (KBr) 3436, 2942, 1725, 1654, 1484, 1366.7, 1255, 1114, 1043, 837, 790, 649 cm^{-1}; HRMS (FAB$^+$) m/e: 271.0998 (MH^+ $C_{10}H_{15}O_5N_4$ requires 271.1026). MO data: E_{LUMO} = −0.942 eV; C^2 (LUMO): 0.195 (C-5, imidazole), 0.189 (N-1, imidazole), 0.172 (C-2, imidazole), 0.152 (N-3, imidazole), 0.127 (N, NO_2), 0.052 and 0.062 (O, NO_2); E_{HOMO} = −10.100 eV; C^2 (HOMO): 0.639 (N, amide), 0.138 (O, amide); total energy: −3515.09111 eV.

Synthesis of methyl 2-(4-nitro-1*H*-1-imidazolyl)acetate (2)

To a solution of 4-nitroimidazole (510 mg, 4.5 mmol) in anhydrous DMF (10 mL), sodium methoxide (500 mg, 9.3 mmol) was added at 90 °C, and then chloroacetic acid methyl ester (573 mg, 5.3 mmol) was added to the reaction mixture and stirred for 2 h at 110 °C. DMF was evaporated under reduced pressure and washed with *n*-hexane to give a pale yellow residue, which was purified by Celite column chromatography (AcOEt) to afford **2** (670 mg, 80%) as a pale yellow solid : mp 129–130 °C; ^{1}H NMR (400 MHz, CD_3OD): δ 3.21 (s, 3H), 4.95 (s, 2H), 7.65 (s, 1H), 8.06 (s, 1H); IR (KBr) 3124, 3022, 297, 1739, 1536, 1489, 1423, 1356, 1291, 1248, 1163, 1142, 983, 914, 841, 786, 765, 656, 645, 592 cm^{-1}; EIMS m/e: 185 (M^+); HRMS (EI$^+$) m/e: 185.0437 (M^+ $C_6H_7O_4N_3$ requires 185.0445).

Synthesis of *N*1-(2-hydroxyethyl)-*N*1-methyl-2-(4-nitro-1*H*-1-imidazolyl)acetamide (TX-1908)

A solution of **2** (370 mg, 1.9 mmol) and *N*-methylethanolamine (200 mg, 2.7 mmol) in anhydrous MeOH (30 mL) was stirred for 23 h at room temperature. The solvent was evaporated under reduced pressure, and the residue was purified by silica gel column chromatography (CH_2Cl_2:MeOH, 9:1) to afford TX-1908 (362 mg, 86%) as a white solid: mp 119–120 °C; ^{1}H NMR (400 MHz, CD_3OD): δ 2.994 and 3.16 (each s, 3H), 3.51–3.55 (m, 2H), 3.69 and 3.77 (each t, J = 5.6 and 5.2 Hz, 2H), 5.16 and 5.24 (each s, 2H), 7.67 (s, 1H), 8.07 and 8.08 (each s, 1H); IR (KBr) 3295, 3119, 2919, 1648, 1537, 1484, 1407, 1337, 1290, 1114, 996, 873, 826, 679 cm^{-1}; HRMS (FAB$^+$) m/e: 228.0865 (M^+ $C_8H_{13}O_4N_4$ requires 228.0859). MO data: E_{LUMO} = −0.697 eV; C^2 (LUMO): 0.389 (C-5, imidazole), 0.149 (N-1, imidazole), 0.063 (C-2, imidazole), 0.147 (C-4, imidazole), 0.074 (N, NO_2);

$E_{HOMO} = -10.410$ eV; C^2 (HOMO): 0.614 (N, amide), 0.135 (O, amide); total energy: −2953.57440 eV.

Synthesis of *N*1-(2-hydroxypropyl)-2-(2-nitro-1*H*-1-imidazolyl)acetamide (TX-1909)

To a solution of **1** (200 mg, 1.1 mmol) in anhydrous MeOH (6 mL), *dl*-isopropanolamine (250 mg, 3.3 mmol) was added. The reaction mixture was refluxed for 15 h. The solvent was evaporated under reduced pressure, and the residue was purified by silica gel column chromatography (CH_2Cl_2:MeOH, 9.5:0.5) to afford TX-1909 (213 mg, 85%) as a white solid: mp 125–126 °C; ^{1}H NMR (400 MHz, CD_3OD): δ 1.15 (d, $J = 6.4$ Hz, 3H), 3.15–3.28 (m, 2H), 3.81–3.85 (m, 1H), 5.18 (s, 2H), 7.16 (s, 1H), 7.44 (s, 1H); IR (KBr) 3307, 3154, 2966, 1666, 1572, 1542, 1495, 1360, 1296, 1260, 1155, 1084, 843, 773, 720 cm^{-1}; HRMS (FAB$^+$) *m*/*e*: 229.0916 (MH^+ $C_9H_{12}O_4N_4$ requires 229.0892). MO data: $E_{LUMO} = -0.946$ eV; C^2 (LUMO): 0.192 (C-5, imidazole), 0.188 (N-1, imidazole), 0.160 (C-2, imidazole), 0.159 (N-3, imidazole), 0.136 (N, NO_2), 0.055 and 0.070 (O, NO_2); $E_{HOMO} = -10.043$; C^2 (HOMO): 0.654 (N, amide), 0.162 (O, amide); total energy: −2953.77667 eV.

Synthesis of methyl 2-(1*H*-1-imidazolyl)acetate (3)

To a solution of imidazole (1 g, 14.7 mmol) and chloroacetic acid methyl ester (1.6 g, 15.0 mmol) in anhydrous DMF (40 mL), triethylamine (2.3 g, 22.7 mmol) was added and stirred for 22 h at 60 °C. The solvent was evaporated under reduced pressure, and the residue was purified by silica gel column chromatography (CH_2Cl_2:MeOH, 9:1) to afford **3** (924 mg, 45%) as colorless needles (from $CHCl_3$): mp 55–56 °C; ^{1}H NMR (400 MHz, CDCl): δ 3.79 (s, 3H), 4.71 (s, 2H), 6.95 (s, 1H), 7.09 (s, 1H), 7.50 (s, 1H); IR (KBr) 3471, 2956, 1751, 1512, 1418, 1374, 1299, 1216, 1073, 990, 907, 829, 761, 692, 663, 573 cm^{-1}; EIMS *m*/*e*: 140 (M^+). HRMS (EI$^+$) *m*/*e*: 140.0587 (M^+ $C_6H_8O_2N_2$ requires 140.0586).

Synthesis of *N*1-(2-hydroxyethyl)-*N*1-methyl-2-(1*H*-1- imidazolyl)acetamide (TX-1910)

A solution of **3** (900 mg, 8 mmol) and *N*-methylethanolamine (1.27 g, 16.8 mmol) in anhydrous MeOH (45 mL) was stirred for 15 h at room temperature. The solvent was evaporated under reduced pressure, and the residue was purified by silica gel column chromatography (CH_2Cl_2:MeOH, 9:1) to afford TX-1910 (828 mg, 56%) as a colorless crystal: mp 145–146 °C; ^{1}H NMR (400 MHz, CD_3OD): δ 2.97 and 3.15 (each s, 3H), 3.49–3.55 (m, 2H), 3.68 and 3.75 (each t, $J = 5.6$ and 5.2 Hz, 2H), 5.03 and 5.12 (each s, 2H), 6.95 (s, 1H), 7.04 and 7.06 (each s, 1H), 7.59 and 7.60 (each s, 1H); IR (KBr) 3186, 2869, 1647, 1488, 1406, 1335, 1300, 1236, 1053, 918, 848, 754 cm^{-1}; HRMS (FAB$^+$) *m*/*e*: 183.0993 (M^+ $C_8H_{13}O_2N_3$ requires 183.1008). MO data: $E_{LUMO} = -0.346$ eV; C^2 (LUMO) 0.475 (N, amide); $E_{HOMO} = -9.415$ eV; C^2 (HOMO): 0.314 (C-4, imidazole), 0.303 (C-5, imidazole), 0.269 (C-2, imidazole), 0.135 (O, amide); total energy: −2222.06461 eV.

Synthesis of 2-{methyl[2-(2-nitro-1*H*-1-imidazolyl)acetyl]-amino}ethyl hydrogen sulfate (TX-1911)

To a solution of TX-1877 (280 mg, 1.2 mmol) in anhydrous pyridine (7 mL), pyridine–sulfur trioxide (206 mg, 1.3 mmol) was added and stirred for 2 h at room temperature. The solvent was evaporated under reduced pressure, and the residue was purified by silica gel column chromatography (CH_2Cl_2:MeOH, 4:6) to give TX-1911 (287 mg, 78%) as a yellow solid: mp 130–132 °C; ^{1}H NMR (400 MHz, CD_3OD): δ 3.00 and 3.25 (each s, 3H), 3.68 (t, $J = 5.2$ Hz, 1H), 3.77 (t, $J = 5.2$ Hz, 1H), 4.12 (t, $J = 5.2$ Hz, 1H), 4.23 (t, $J = 5.2$ Hz, 1H), 5.45, 5w > 5.48 and 5.57 (each s, 2H), 7.14–7.49 (each s, total 2H); IR (KBr) 3471, 2954, 1654, 1490, 1366, 1237, 1143, 1067, 1014, 902, 773, 643, 579 cm^{-1}. Anal. calcd for $C_8H_{12}0_7N_4S{\cdot}2.5H_2O$: C, 27.19; H, 3.42; N, 15.85. Found: C, 27.23; H, 3.52; N, 15.43. MO data: $E_{LUMO} = -0.946$ eV; C^2 (LUMO): 0.194 (C-5, imidazole), 0.188 (N-1, imidazole), 0.163 (C-2, imidazole), 0.157 (N-3, imidazole), 0.131 (N, NO_2), 0.055 and 0.069 (O, NO_2); $E_{HOMO} = -10.043$ eV; C^2 (HOMO): 0.661 (N, amide), 0.127 (O, amide); total energy: −4021.04278 eV.

Synthesis of *N*1-ethyl-*N*1-methyl-2-(2-nitro-1*H*-1-imidazolyl)acetamide (TX-1914)

A solution of **1** (70 mg, 0.35 mmol) in *N*-ethylmethylamine (0.5 mL, 5.8 mmol) was stirred for 24 h at room temperature. The reaction mixture was evaporated in vacuo to give an oil residue, which was purified by silica gel column chromatography (CH_2Cl_2:MeOH, 9.5:0.5), to afford TX-1914 (74 mg, 91%) as a white solid: mp 74–75 °C; ^{1}H NMR (400 MHz, $CDCl_3$): δ 1.14 and 1.33 (each t, $J = 7.2$ Hz, 3H), 2.97 and 3.10 (each s, 3H), 3.40–3.48 (m, 2H), 5.18 and 5.23 (each s, 2H), 7.06 (s, 1H), 7.18 (s, 1H); IR (KBr) 3421, 2968, 1654, 1540, 1508, 1490, 1457, 1414, 1363, 1298, 1163, 1143, 1090, 845, 815, 797, 668 cm^{-1}; HRMS (FAB$^+$) *m*/*e*: 213.0993 (M^+ $C_8H_{12}O_3N_4$ requires 213.0988). MO data: $E_{LUMO} = -0.929$ eV; C^2 (LUMO): 0.195 (C-5, imidazole), 0.190 (N-1, imidazole), 0.170 (C-2, imidazole), 0.153 (N-3, imidazole), 0.128 (N, NO_2), 0.054 and 0.067 (O, NO_2); $E_{HOMO} = -10.013$ eV; C^2 (HOMO): 0.655 (N, amide), 0.142 (O, amide); total energy: −2659.81336 eV.

Synthesis of 1-(4-methylpiperazino)-2-(2-nitro-1*H*-1-imidazolyl)-1-ethanone (TX-1920)

A solution of **1** (200 mg, 1.1 mmol) in *N*-methylpiperazine (0.5 mL, 4.5 mmol) was stirred for 72 h at room temperature. *N*-Methylpiperazine was evaporated in vacuo, and the brown residue was purified by aluminum oxide (Al_2O_3 neutral, 70–230 mesh, Merck) column chromatography (CH_2Cl_2:MeOH, 95:5) to afford TX-1920 (220 mg, 79%) as an amorphous brown solid: ^{1}H NMR(400 MHz, CD_3OD): δ 2.25 and 2.26 (each s, 3H), 2.37(m, 2H), 2.47 (m, 2H), 3.51 (m, 4H), 5.35 (s, 2H), 7.06 (s, 1H), 7.30 (s, 1H); IR (KBr) 3455, 2944, 2800, 1654, 1540, 1492.0, 1465, 1428, 1366, 1292, 1257, 1237, 1144, 1074, 1036, 1001, 917, 842, 813 783, 650 cm^{-1};

HRMS (FAB$^+$) *m/e*: 253.1175 (M$^+$ $C_{10}H_{16}O_3N_5$ requires 253.1175). MO data: $E_{LUMO} = -0.994$ eV; C^2 (LUMO): 0.194 (C-5, imidazole), 0.189 (N-1, imidazole), 0.164 (C-2, imidazole), 0.157 (N-3, imidazole), 0.123 (N, NO_2), 0.055 and 0.068 (O, NO_2); $E_{HOMO} = -9.459$ eV; C^2 (HOMO): 0.712 (N, piperazine); total energy: −3105.28588 eV.

Synthesis of 1-morpholino-2-(2-nitro-1*H*-1-imidazolyl)-1-ethanone (TX-1921, Ro 07-1113)

A solution of **1** (200 mg, 1.1 mmol) in morpholine (0.5 mL, 5.7 mmol) was stirred for 87 h at room temperature. The residue was purified by silica gel column chromatography (CH_2Cl_2:acetone, 8:2) to afford TX-1921 (220 mg, 83%) as a light yellow solid: mp 114–115 °C (lit.[33] mp 113.5–115°C); ^{1}H NMR (400 MHz, $CDCl_3$): δ 3.55–3.79 (8H), 5.22 (s, 2H), 7.08 (s, 1H), 7.18 (s, 1H); IR (KBr) 3441, 3147, 2972, 2855, 2362, 1655, 1536, 1491, 1426, 1369, 1292, 1269, 1231, 1215, 1138, 1104, 1065, 1034, 964, 914, 883, 834, 779, 625 cm^{-1}; HRMS (FAB$^+$) *m/e*: 240.0859 (M$^+$ $C_9H_{12}O_4N_4$ requires 240.0845). MO data: $E_{LUMO} = -1.074$ eV; C^2 (LUMO): 0.193 (C-5, imidazole), 0.183 (N-1, imidazole), 0.168 (C-2, imidazole), 0.159 (N-3, imidazole), 0.1280 (N, NO_2), 0.054 and 0.067 (O, NO_2); $E_{HOMO} = -9.459$ eV; C^2 (HOMO): 0.609 (N, amide), 0.132 (O, amide); total energy: −3071.66914 eV.

Synthesis of methyl 2-(4-methyl-1*H*-1-imidazolyl) acetate (4)

To a solution of 4-methylimidazole (410 mg, 5 mmol) in anhydrous DMF (8 mL), potassium *tert*-butoxide (617 mg, 5.5 mmol) was added at 70 °C, then chloroacetic acid methyl ester (596 mg, 5.5 mmol) was added and stirred for 1 h at 90 °C. The solvent was evaporated under reduced pressure, and the residue was purified by silica gel column chromatography (CH_2Cl_2:MeOH, 9.5:0.5), to afford **4** (421 mg, 55%) as a light yellow oil: ^{1}H NMR (400 MHz, $CDCl_3$): δ 2.16 and 2.23 (each s, 3H), 3.78 (s, 3H), 4.61 and 4.63 (each s, 2H), 6.65 and 6.81 (each s, 1H), 7.38 and 7.43 (each s, 1H); IR (KBr) 3354, 1748, 1566, 1501, 1437, 1354, 1290, 1225, 1002, 826.1, 779, 702, 661, 620, 573 cm^{-1}; EIMS *m/e*: 154 (M$^+$); HRMS (EI$^+$) *m/e*: 154.0735 (M$^+$ $C_7H_{10}O_2N_2$ requires 154.0742).

Synthesis of *N*1-(2-hydroxyethyl)-*N*1-methyl-2-(4-methyl-1*H*-1-imidazolyl)acetamide (TX-1931)

A solution of **4** (200 mg, 1.3 mmol) and *N*-methylethanolamine (196 mg, 2.6 mmol) in anhydrous DMF (3 mL) was stirred for 23 h at 70–80 °C. The solvent was evaporated under reduced pressure, and the residue was purified by aluminum oxide (Al_2O_3 neutral, 70–230 mesh, Merck) column chromatography (eluted from CH_2Cl_2 to CH_2Cl_2:MeOH, 9.5:0.5) to afford TX-1931 (101 mg, 51%) as a white solid: mp 119–120 °C; ^{1}H NMR (400 MHz, CD_3OD): δ 2.18 and 2.20 (each s, 3H), 2.94 and 3.10 (each s, 3H), 3.43–3.54 (m, 4H), 4.66 and 4.86 (each s, 2H), 6.65 (s, 1H), 7.26 (s, 1H); IR (KBr) 3423, 2935, 1653, 1508, 1411, 1341, 129, 1235, 1173, 1129, 1050, 1009, 970, 810 cm^{-1}; FABMS *m/e*: 198 (MH$^+$). HRMS (FAB$^+$) *m/e*: 198.1241 (M$^+$ $C_9H_{16}O_2N_3$ requires 198.1243). MO data: $E_{LUMO} = -0.372$ eV; C^2 (LUMO): 0.475 (C, amide), 0.240 (O, amide), 0.072 (N, amide); $E_{HOMO} = -9.132$ eV; C^2 (HOMO): 0.319 (C-4, imidazole), 0.186 (C-2, imidazole), 0.256 (C-5, imidazole), 0.140 (N-1, imidazole); total energy: −2371.782600 eV.

Electrochemical measurements

Cyclic voltammetry (CV) was carried out with an ALS/chi Electrochemical Analyzer Model 660A, BAS, with a three-electrode system. A glassy-carbon as a working electrode, Pt-wire as an auxiliary electrode, and Ag/AgCl (saturated sodium chloride) as a reference electrode were used. The reference electrode was separated from the bulk of the solution by a glass frit and was immersed in an aqueous solution containing 0.1 M-phosphate buffer (0.1 M, pH = 7.4)−0.5% (v/v) DMSO. All experiments were measured at 298 K in each sample solution (1 mM, 500 μL) purged with N_2 gas. The cathodic peak potential (E_{pc}) was evaluated versus Ag/AgCl, in which the sweep rate was 100 mV/s for CV. The potentials of both reference electrodes Ag/AgCl and NHE (normal hydrogen electrode) were calibrated by the following equation: E(NHE) = E(Ag/AgCl) + 212 mV.

In vitro radiosensitizing assay

In vitro radiosensitization was measured in EMT6/KU single cells under hypoxic conditions. Hypoxic cell radiosensitizer was added to an EMT6/KU cell (5×10^5 cells/mL) suspension at a dose of 1 mM in test tubes and treated with 95% N_2–5%CO_2 gas for 15 min. Local irradiation of 8–32 Gy was given by ^{60}Co γ-rays for 30 min after the administration and then colony forming assays were performed. Enhancement ratios (ERs) were determined from the ratio of radiation doses required to reduce the surviving fraction of EMT6/KU cells to 1%. Usually, each ER was obtained from survival curves consisting of four or five points per curve.

In vivo radiosensitization, tumor growth inhibition, suppression of lung metastasis, and mononuclear cells infiltration

In vivo radiosensitizing activity, tumor growth inhibition, suppression of lung metastasis, and immunopotentiation were evaluated as reported previously.[17] In brief, female C3H/He mice bearing the SCCVII tumor were used. Fifteen or 10 days after the inoculation of 10^5 SCCVII tumor cells into the right hind thigh of the animals at 8 weeks of age, a drug (0.4 mg/g) was administered i.p. and then local irradiation of 30 Gy was given by ^{60}Co γ-rays for 30 min after the administration. The tumor volume was measured at three perpendicular diameters with 2- or 3-day intervals. The relative tumor volume was compared to the tumor volume (1.00) at the beginning of the treatment. Mice were sacrificed after the drug treatment to count the number of metastatic nodules on the surface of the lungs. All tissues were stained by the ABC method for immunological evaluation.

Acknowledgements

The authors thank Dr. Yoshihiro Takekawa and Dr. Hiroshi Maezawa of the School of Medical Sciences, The University of Tokushima for generous help with the radiobiological experiments. The authors also thank Mrs. Maki Nakamura, Mrs. Emiko Okayama, Mrs. Kayoko Yamashita and the staff of the Center for Cooperative Research of our Faculty for measurement of NMR, MS and elemental analysis. We also appreciate Dr. Hiroshi Terada, Dr. Yasuo Shinohara, and Mrs. Yasuko Yoshioka of the Faculty of Pharmaceutical Sciences of The University of Tokushima, for measurement of HRMS.

References and Notes

1. Gazit, Y.; Baish, J. W.; Safabakhsh, N.; Leunig, M.; Baxter, L. T.; Jain, R. K. *Microcirculation* **1997**, *4*, 395.
2. Teicher, B. A. *Cancer Metastasis Rev*. **1994**, *13*, 139.
3. Tomida, A.; Tsuruo, T. *Anti-Cancer Drug Des*. **1999**, *14*, 169.
4. Brown, J. M. *Cancer Res*. **1999**, *59*, 5863.
5. Hori, H.; Nagasawa, H.; Terada, H. In *Advances in Environmental Science and Technology: Oxidants in the Environment;* Nriagu, J. O.; Simmons, M. S., Eds.; John Wiley: New York, 1994; Vol. 28, pp 425–443.
6. Paulson, O. B.; Melgaard, B.; Hansen, H. S.; Kamieniecka, Z.; Kohler, O.; Hansen, J. M.; Pedersen, A. G.; Tang, X.; Trojaborg, W. *Acta Neurol. Scand. (Suppl.)* **1984**, *100*, 133.
7. Kanclerz, A.; Chapman, J. D. *Int. J. Radiat. Oncol. Biol. Phys*. **1988**, *14*, 309.
8. Hori, H.; Murayama, C.; Mori, T.; Shibamoto, Y.; Abe, M.; Onoyama, Y.; Inayama, S. *Int. J. Radiat. Oncol. Biol. Phys*. **1989**, *16*, 1029.
9. Nagasawa, H.; Bando, M.; Hori, H.; Satoh, T.; Tada, T.; Onoyama, Y.; Inayama, S. *Int. J. Radiat. Oncol. Biol. Phys*. **1992**, *22*, 561.
10. Denny, W. A.; Wilson, W. R.; Hay, M. P. *Br. J. Cancer* **1996**, *74*, S32.
11. Brown, J. M.; Amato, J. G. *Cancer Res*. **1998**, *58*, 1408.
12. Shweiki, D.; Itin, A.; Soffer, D.; Keshet, E. *Nature* **1992**, *359*, 843.
13. Hori, H.; Jin, C.-Z.; Kiyono, M.; Kasai, S.; Shimamura, M.; Inayama, S. *Bioorg. Med. Chem*. **1997**, *5*, 591.
14. Nagasawa, H. *Advance in Pharmaceutical Sciences, Vol. 10*. Tokyo, Japan: The Res. Fund. Pharm. Sci., 1994; Vol. 10, p 147.
15. Inomata, T.; Ogawa, Y.; Nishioka, A.; Hamada, N.; Ito, S.; Kariya, S.; Yoshida, S.; Nagasawa, H.; Hori, H.; Inayama, S. *Oncol. Rep*. **1999**, *6*, 1209.
16. Inomata, T.; Ogawa, Y.; Itoh, S.; Kariya, S.; Hamada, N.; Nishioka, A.; Yoshida, S.; Nagasawa, H.; Hori, H.; Inayama, S. *Int. J. Mol. Med*. **1999**, *4*, 257.
17. Kasai, S.; Nagasawa, H.; Kuwasaka, H.; Oshodani, T.; Inomata, T.; Nishioka, A.; Ogawa, Y.; Yoshida, S.; Inayama, S.; Hori, H. *Int. J. Radiat. Oncol. Biol. Phys*. **1998**, *42*, 799.
18. Brown, J. M.; Workman, P. *Radiat. Res*. **1980**, *82*, 171.
19. Adams, G. E.; Flockhart, I. R.; Smithen, C. E.; Stratford, I. J.; Wardman, P.; Watts, M. E. *Radiat. Res*. **1976**, *67*, 9.
20. Inayama, S.; Hori, H.; Ohsaka, T.; Mori, T.; Shibata, C. *Gann (Jpn. J. Cancer Res.)* **1981**, *72*, 156.
21. Sundfor, K.; Lyng, H.; Rofstad, E. K. *Br. J. Cancer* **1998**, *78*, 822.
22. Stratford, M. R. L.; Dennis, M. F.; Margaret, B. A.; Watts, E.; Watf, R. R.; Woodcock, M. *Int. J. Radiat. Biol*. **1989**, *16*, 1007.
23. Wallace, P. K.; Morahan, P. S. *J. Leukoc. Biol*. **1994**, *56*, 41.
24. Konovalova, N. P.; Volkova, L. M.; Tatyanenko, L. V.; Kotelnikova, R. A.; Yakushchnko, T. N.; Kagiya, T. V. *Neoplasma* **1997**, *44*, 361.
25. Tcherdyntseva, N. V.; Kokorev, O. V.; Konovalova, N. P.; Kagiya, T. V. *Sensitization Newsletter* **1998**, *5*, 2.
26. Kanclerz, A.; Chapman, J. D. *Int. J. Radiat. Oncol. Biol. Phys*. **1988**, *14*, 309.
27. Iwakawa, M.; Tofilon, P. J.; Hunter, N.; Stephens, L. C.; Milas, L. *Clin. Exp. Metastasis* **1987**, *5*, 289.
28. Greco, C.; Del Bufalo, D.; Giannarelli, D.; Marangolo, M.; Fuggetta, M. P.; Bonmassar, E.; Zupi, G. *Clin. Exp. Metastasis* **1990**, *8*, 153.
29. Hyland, R.; Gescher, A.; Thummel, K.; Schiller, C.; Jheeta, P.; Mynett, K.; Smith, A. W.; Mraz, J. *Mol. Pharmacol*. **1992**, *41*, 259.
30. Overton, M.; Hickman, J. A.; Threadgill, M. D.; Vaughan, K.; Gescher, A. *Biochem. Pharmacol*. **1985**, *34*, 2055.
31. Fujita, T.; Iwasa, J.; Hansch, C. *J. Am. Chem. Soc*. **1964**, *86*, 5175.
32. Stewart, J. J. P. *J. Comput. Chem*. **1989**, *10*, 209.
33. Beaman, A. G.; Tautz, W.; Duschinsky, R. *Antimicrob. Agents Chemother*. **1967**, *7*, 520.